



Highly sensitive sensing of Fe(III) harnessing Schiff based ionophore: An electrochemical approach supported with spectroscopic and DFT studies

Sarbjeet Kaur, Bilal Ahmad Shiekh, Damanjit Kaur, Inderpreet Kaur *

Department of Chemistry, Centre for Advanced Studies, Guru Nanak Dev University, Amritsar, Punjab 143005, India

ARTICLE INFO

Article history:

Received 2 December 2020

Revised 15 March 2021

Accepted 19 March 2021

Available online 25 March 2021

Keywords:

Fe³⁺ detection

Schiff base

Voltammetric sensor

Carbon paste electrode

Potentiometric sensor

DFT studies

ABSTRACT

The vital role of iron in biological systems and health implications posed to humans due to associated toxicity by the consumption of iron contaminated food or drinking water and exposure to other environmental sectors demand sensitive methods for its determination in various medicinal, biological and environmental samples. In the current work, a potent Schiff-base ionophore 1,1'-((ethane-1,2-diylbis(oxy))bis(2,1-phenylene))bis(N-p-tolylmethanimine) (**SB**) was synthesized and analysed for its redox behaviour using cyclic voltammetry (CV) and differential pulse voltammetry (DPV) followed by its application for development of Fe³⁺ sensing methods. The voltammetric sensor exhibited sensitivity towards Fe³⁺ in the linear concentration range of 1–19 µM with a detection limit of 5.57×10^{-8} M. The carbon paste electrode incorporating **SB** (CPE-**SB**) showed sensitive potentiometric response for Fe³⁺ with a Nernstian slope of 18.6 ± 0.2 mV/decade over a wide concentration range of 1.0×10^{-7} – 1.0×10^{-2} M with a detection limit of 5.0×10^{-8} M. Furthermore, UV-Vis and fluorescence studies confirmed the binding of **SB** with Fe³⁺ and found to exhibit the detection limits of 0.56 µM and 0.98 µM, respectively. Large binding constant (1.01×10^4 M⁻¹) and negative free energy (-22.84 kJmol⁻¹) calculated using Benesi-Hildebrand (BH) equation confirmed 1:1 complexation between **SB** and Fe³⁺ which was also validated by Job's plot and mass spectrometry. DFT studies also confirmed the structure of **SB**-Fe³⁺ complex with reduction in HOMO-LUMO gap from 4.11 eV to 1.08 eV. CPE-**SB** electrode was successfully applied for the estimation of Fe³⁺ in real samples such as ground water, surface water and pharmaceutical samples.

© 2021 Elsevier B.V. All rights reserved.

1. Introduction

Iron is well recognised for its vital role in physiological processes for living beings such as oxygen transport, cellular metabolism, transcriptional regulation and enzymatic reactions [1,2]. It is present as Fe²⁺ and Fe³⁺ in the dissolved state and transformation between the two oxidation states commonly occurs. It is necessary to maintain the iron content up to appropriate level in human body as its deficiency causes immunodeficiency disorders such as anaemia which include fatigue, pale skin, shortness of breath, drowsiness, weakness and low blood pressure, whereas iron overload leads to medical disorders such as cardiac arrest, cell damage, Alzheimer's disease, Hepatitis, Parkinson's disease, Hemochromatosis, cancer, diabetes, etc [3–8]. According to World Health Organization (WHO), maximum permissible limit of iron in drinking water is 2 mg/L [9]. Besides, iron is widely used in industrial sectors including water pipe, plastic, steel, paint industries and medical application which leads to its permeation into the environment (water

and soil) and contribute to the disturbance in ecological balance [10]. Thus, in the present epoch, qualitative and quantitative determination of iron content in different environmental and biological samples gained extraordinary attention all over the world.

In last two decades, various organic compounds like crown ethers [11], cryptands [12], porphyrins [13], calixarenes [14], macrocyclic assemblies [15], Schiff bases [16], modified conducting polymers [17] etc. have been explored for their applications in the development of sensing methods for determination of various potentially toxic elements. Among various ionophores, Schiff bases are versatile ligands as they offer advantages such as thermal stability, flexible synthesis, capacity for complex formation with metal ions; medicinal and biological properties [18]. Schiff bases favour the interaction with transition metal ions through π electrons of the C = N group. Furthermore, the presence of donor atoms like O and N in Schiff bases also allows the formation of stable complexes via strong coordination bonding between ligand and metal ions. The chelation with transition metal ions may lead to enhancement of ICT (intramolecular charge transfer) transition or LMCT (ligand-to-metal charge-transfer) which are being utilized for the sensing of transition metal ions [19,20]. Further the diverse

* Corresponding author.

E-mail address: inderpreet11@yahoo.co.in (I. Kaur).

nature of the Schiff bases can be revealed from their significant applications in different areas of electrochemistry, optical sensing and biological analysis [21–24].

Several reports in literature addressed the application of Schiff based ionophores for determination of Fe^{3+} using various techniques such as voltammetry [25,26], potentiometry utilizing polymer membrane electrodes [27,28], spectrophotometry [29,30] and fluorescence spectroscopy [31,32] but the reports describing voltammetric detection of Fe^{3+} using Schiff base ionophore are quite limited. Thus, to design simple, fast, cheap and reliable methods for detection of metal ions in biological, environmental and chemical fields using Schiff base ligand is coveted. Moreover, electrochemical methods such as voltammetry and potentiometry are associated with many advantages such as portability, accuracy, easy operation, low cost, no requirement of sample pre-treatment and direct quantification of analyte in real samples which makes them superior and promising techniques for trace analysis [33].

Keeping in view the properties of Schiff bases and advantages associated with electrochemical techniques, the present work was planned with aim to synthesize Schiff base 1,1'-((ethane-1,2-diylbis(oxy))bis(2,1-phenylene))bis(N-p-tolylmethanimine) (**SB**) followed by its application for sensitive and selective detection of Fe^{3+} ions using electroanalytical techniques: Differential pulse voltammetry (DPV) and Potentiometry. Further, spectroscopic studies using UV–Visible and fluorescence were employed to support the binding behaviour of **SB** with Fe^{3+} . In order to explore the sensing capability of **SB** for onsite monitoring of Fe^{3+} content in various samples, **SB** based carbon paste electrode was fabricated and subjected to potentiometric sensing of Fe^{3+} ions in real samples after simple pre-treatment.

2. Experimental

2.1. Materials

Salicylaldehyde and 1,2-dibromoethane and p-toluidine were purchased from Spectrochem, India. Potassium carbonate and high viscosity paraffin oil (density = 0.840 g/cm^3) were obtained from Fischer Scientific and Merck, respectively. Graphite powder (GP), tetrabutylammonium perchlorate (TBAP) and metal perchlorates were procured from Sigma Aldrich and used without any further purification. All other reagents and solvents used were of analytical grade. Double distilled water (DDW) was used for preparing the standard stock solutions and carrying out further dilutions wherever required.

2.2. Synthesis and characterization of 1,1'-((ethane-1,2-diylbis(oxy))bis(2,1-phenylene))bis(N-p-tolylmethanimine) (**SB**)

SB was synthesized following two steps procedure as described in Scheme 1. In the first step, 2,2'-(ethane-1,2-diylbis(oxy))dibenzaldehyde was synthesized as described by Ilhan et al. [34]. In brief, the solution of salicylaldehyde (0.1 mol) and potassium carbonate (0.05 mol) in DMF was stirred, into which 1,2-dibromoethane (0.05 mol in DMF) was added drop wise. The reaction mixture was refluxed at 150°C for 10 h and then refluxing was continued for 5 h at room temperature. The progress of reaction was monitored using TLC and after completion of the reaction, double distilled water was added and the reaction mixture was kept in the refrigerator for 1 h. The precipitates of 2,2'-(ethane-1,2-diylbis(oxy))dibenzaldehyde so obtained were filtered, washed with water and then dried in the vacuum. In second step, the Schiff base (**SB**) was prepared by condensation reaction of 2,2'-(ethane-1,2-diylbis(oxy))dibenzaldehyde (0.05 mol) and p-toluidine (0.1 mol)

in ethanol. The reaction mixture was refluxed for 6 h and on completion of reaction, the solid product was filtered, washed with cold ethanol and subjected to vacuum drying. The ionophore (**SB**) was characterized using ^1H NMR, ^{13}C NMR, FT-IR and Mass spectroscopy (S1–S4). Yield = 79%. ^1H NMR (400 MHz, CDCl_3) δ /ppm: 2.34 (6H, s, $-\text{CH}_3$), 4.45 (4H, br, $-\text{CH}_2-$), 6.98–7.13 (12H, m, ArH), 7.37–7.41 (2H, m, ArH), 8.13–8.15 (2H, dd, ArH), 8.86 (2H, s,). ^{13}C NMR (100 MHz, CDCl_3) δ /ppm: 21.09, 67.29, 112.49, 121.01, 121.63, 125.40, 127.78, 129.76, 132.59, 135.61, 150.09, 155.45, 158.52. HRMS: m/z calculated for $\text{C}_{30}\text{H}_{28}\text{N}_2\text{O}_2$: 448.2151 Found: 449.2020 ($\text{M}^+ + 1$). IR (KBR) $\nu_{\text{max}}/\text{cm}^{-1}$: $\nu_{\text{Ar-C-H}}$ = 3041, $\nu_{\text{Ar-C=C}}$ = 1595, $\nu_{\text{C-H}}$ = 2944, $\nu_{\text{C-O}}$ = 1244, $\nu_{\text{C=N}}$ = 1684, $\nu_{\text{C-H}}$ (bend) = 1356.

2.3. Voltammetric measurements

The cyclic voltammetric (CV) and differential pulse voltammetric (DPV) measurements were performed on Autolab PGSTAT302N Metrohm workstation, using glass cell with three-electrode assembly, i.e. platinum electrode (diameter 2 mm) as working electrode, Ag/AgCl as reference electrode and platinum wire as counter electrode. NOVA 2.0 software was used to record and collect the data. Before measurements, the surface of platinum working electrode was cleaned by polishing with $0.05\text{-}\mu\text{m}$ alumina followed by ultrasonication in acetonitrile. The CV and DPV studies were carried out in the potential range from 0.5 V to 2.0 V using 0.01 molL^{-1} TBAP and acetonitrile (CH_3CN) as a supporting electrolyte and solvent, respectively. Nitrogen gas (99.99% high purity) was used for purging the contents in electrochemical cell for 10 min prior to each electrochemical measurement to create an inert environment. The cell assembly was placed in a Faraday cage to avoid any kind of external interference. All the electrochemical measurements were performed at an ambient temperature of $25.0 \pm 1^\circ\text{C}$.

2.4. Fabrication of SB based carbon paste electrode (CPE)

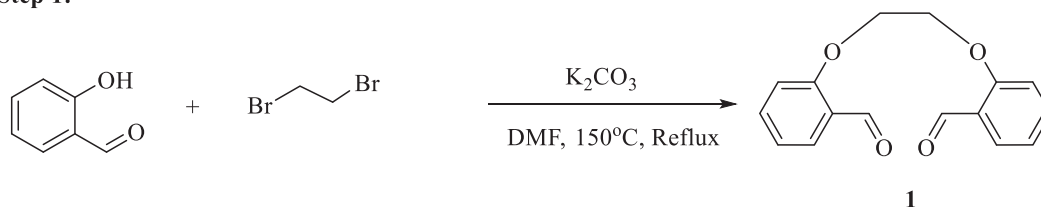
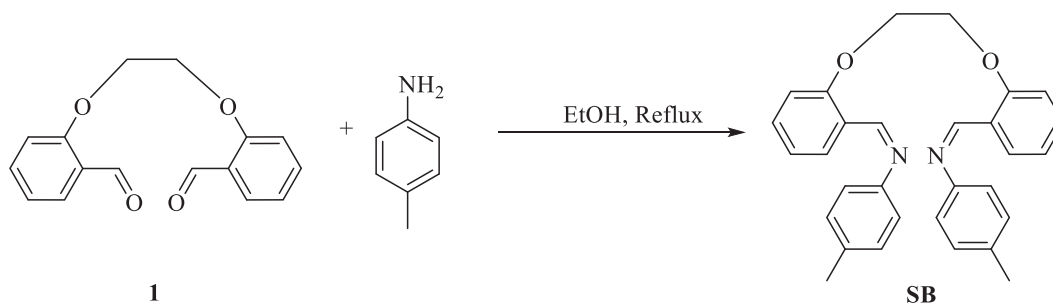
For the preparation of carbon paste electrode (CPE), **SB** was used as a modifier. For this, graphite powder (64 mg), ionophore **SB** (10 mg) and paraffin oil (26 mg) were mixed thoroughly using mortar pestle. The paste so obtained was then packed firmly into the blank electrode (Metrohm, diameter 2 mm) and allowed to dry at the room temperature. The modified CPE (CPE-**SB**) was polished on polishing paper to obtain a shiny surface by removing extra composite material attached. The surface of prepared CPE-**SB** was preconditioned in $1.0 \times 10^{-2} \text{ M}$ Fe^{3+} solution for 24 h. The electrode was removed from the preconditioning solution, rinsed with double distilled water and used as working electrode for potentiometric measurements.

2.5. Potentiometric studies

The potentiometric measurements were performed on Autolab PGSTAT302N Metrohm workstation using CPE-**SB** as a working electrode and Ag/AgCl as a reference electrode. The performance of the electrode was examined by measuring the electromotive force (EMF) of Fe^{3+} solution in the concentration range from $1.0 \times 10^{-10} \text{ M}$ to $1.0 \times 10^{-2} \text{ M}$ using the following electrochemical cell assembly:

CPE – **SB** | Sample solution (Fe^{3+} solution) || Ag/AgCl(s), KCl (3M)

All measurements were performed at $25.0 \pm 1^\circ\text{C}$. The pH of the solutions was monitored using Contech CPH-103 pH meter with a conventional glass pH electrode.

Step 1:**Step 2:****Scheme 1.** Synthetic pathway for 1,1'-((ethane-1,2-diylbis(oxy))bis(2,1-phenylene))bis(N-p-tolylmethanimine) (SB).**2.6. Spectroscopic studies**

The UV–Visible spectra were recorded using Shimadzu 1601 spectrophotometer in the range of 200–600 nm using a quartz cuvette (path length of 1 cm). Fluorescence spectra were recorded on Hitachi F-4600 spectrofluorimeter in the range of 335–450 nm at an excitation wavelength of 320 nm using an excitation-emission slit width of 5 nm. All UV–Vis and fluorescence titrations were performed using 5 μ M solution of **SB** in CH_3CN . ^1H and ^{13}C NMR spectra were recorded on JEOL 400 MHz using CDCl_3 as a solvent. FTIR spectra were obtained using Cary 630 FT-IR (Agilent Technologies) while high-resolution mass spectra were recorded using BRUKER DALTONIK microTOF-Q11 spectrometer.

2.7. Computational details

In order to establish the sensitivity of **SB** towards Fe^{3+} , TD-DFT calculations were carried out employing B3LYP-D3 density functional theory in conjunction with 6-31G(d,p) basis set for all atoms except for Fe for which MDF10 ECPs basis set and pseudo potential were used. All the geometry optimizations of complexes without any truncations have been performed at above mentioned level of theory followed by Harmonic frequency calculations to confirm that the optimized complexes are true minima on potential energy surface. Solvent effects have been introduced using Integral Equation Formalism Polarizable Continuum Model IEFPCM/SMD solvation model in Acetonitrile at normal temperature. All the above mentioned calculations have been performed using Gaussian 09 suite of Programmes [35].

2.8. Sample preparation for real application**2.8.1. Determination of Fe^{3+} in water samples**

For the determination of Fe^{3+} content in real samples, ground and surface water samples were collected from various locations of Amritsar, Punjab. The samples so collected were filtered through Whatman filter paper no. 42 to remove the solid impurities. For the conversion of Fe^{2+} present in the real sample into Fe^{3+} , the samples were subjected to oxidation using 1% H_2O_2 and concentrated HNO_3 with pH maintained below 2 [25]. The samples were then sub-

jected to the determination of Fe^{3+} content using CPE-**SB**. For the sake of comparison, same samples were subjected to estimation of Fe^{3+} content using well established technique i.e. Microwave Plasma Atomic Emission Spectroscopy (MPAES).

2.8.2. Determination of Fe^{3+} in pharmaceutical samples

In order to explore application of CPE-**SB** in pharmaceutical analysis, the synthetic samples were prepared using pharmaceutical tablets of known compositions. For the preparation of samples, tablets were first ground into powder and then 1 g of the powdered tablet was dissolved in minimum amount of concentrated HNO_3 . Further, to oxidize Fe^{2+} to Fe^{3+} , 5 mL of 1% H_2O_2 was added to the sample solution followed by pH adjustment to 2 using HNO_3 . The samples so prepared were filtered and diluted to 100 mL using double distilled water followed by determination of Fe^{3+} content using CPE-**SB** and MPAES.

3. Results and discussion

SB was synthesized via condensation of 2,2'-(ethane-1,2-diylbis(oxy))dibenzaldehyde (**1**) and p-toluidine. The structural feature of **SB** consists of pseudo-cavity that can accommodate metal ions via coordination through N and O donor atoms present in it which is prerequisite for sensing. In order to explore its electrochemical sensing potential, **SB** was subjected to voltammetric and potentiometric studies and results so obtained are discussed in following sections:

3.1. Voltammetric measurements**3.1.1. Electrochemical behaviour of SB**

The voltammetric studies were aimed to investigate the redox performance of **SB** (5×10^{-4} M) in CH_3CN containing 0.01 M TBAP as supporting electrolyte using cyclic voltammetry (CV) and differential pulse voltammetry (DPV). The CV of **SB** exhibits three irreversible anodic peaks at 1.58 V, 1.13 V and 0.89 V in the potential range from 0.5 V to 2.0 V vs. Ag/AgCl at the scan rate of 50 mV/s as shown in Fig. 1(a). The peak at 1.58 V may be attributed to O atoms while the peaks at 1.13 V and 0.89 V may be assigned to N atoms of imine groups in **SB** molecule [36]. Similarly, three

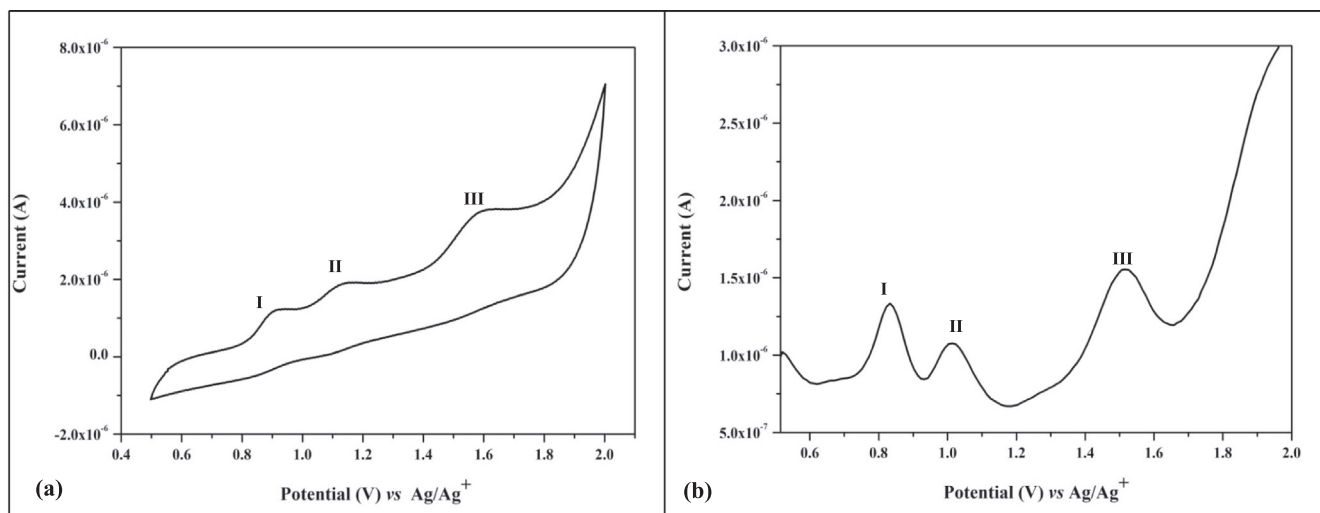


Fig. 1. (a) Cyclic Voltammogram (CV) of pure receptor SB (5×10^{-4} M in CH_3CN). Supporting electrolyte: TBAP (0.01 M), Scan rate: 50 mV/sec; (b) Differential Pulse Voltammogram (DPV) of pure receptor SB (5×10^{-4} M in CH_3CN); Supporting electrolyte: TBAP (0.01 M), Pulse amplitude: 0.05 V, Pulse width: 0.05 s, Pulse period: 0.5 s.

distinct anodic peaks at 1.50 V, 1.02 V and 0.83 V were also observed when **SB** was subjected to DPV measurements (Fig. 1 (b)). The results obtained from CV and DPV measurements in preliminary investigation confirmed the redox behaviour of **SB** which could allow one to conclude that it could serve the purpose of electrochemical sensing.

3.1.2. Interaction of SB with metal ions

To study the complexation behaviour of **SB** towards diverse metal ions, differential pulse voltammetry (DPV) was performed as it offers an advantage of well-defined and sharper current peaks than CV under identical conditions. Upon addition of different metal ions solutions (25 μM) such as alkali (Na^+ , Li^+), alkaline (Ca^{2+}) and transition metal ions (Ni^{2+} , Zn^{2+} , Cd^{2+} , Co^{2+} , Pb^{2+} , Cu^{2+} , Fe^{2+} , Fe^{3+} , Al^{3+} and Cr^{3+}) into **SB** solution (5×10^{-4} M), no major shift in positions and heights of various peaks was observed except Fe^{3+} (Fig. 2(a)). With Fe^{3+} , there is complete quenching of peak current at 1.50 V while other two peaks at 1.02 V and 0.83 V showed

enhancement in peak current values under similar conditions with a remarkable shift of the peak at 1.02 V towards more positive potential as shown in Fig. 2(a). Similar quenching of peak at 1.58 V and enhancement in peak current at 0.89 V were observed in CV studies as expected, while the peak at 1.13 V showed anodic shift along with the increase in current parameter indicating the formation of **SB**- Fe^{3+} complex (Fig. 2(b)).

The favourable behaviour of **SB** for complexation with only Fe^{3+} in comparison to other metal ions under investigation can be explained on the basis of the fact that **SB** contains $\text{C}=\text{N}$ and $-\text{O}-$ moieties that are associated with hard properties and prefer to bind hard metal ions. Among the various metal ions tested, Ni^{2+} , Zn^{2+} , Co^{2+} , Pb^{2+} , Cu^{2+} , Fe^{2+} are borderline acids and Cd^{2+} is soft acid, so these ions are not expected to bind with **SB** so effectively. Although Na^+ , Li^+ , Ca^{2+} , Cr^{3+} and Al^{3+} are hard but their charge density values ($\rho_{\text{Na}^+} = 0.26$; $\rho_{\text{Li}^+} = 0.59$; $\rho_{\text{Ca}^{2+}} = 0.49$; $\rho_{\text{Cr}^{3+}} = 2.18$) are less than that of Fe^{3+} ($\rho_{\text{Fe}^{3+}} = 4.30$) and Al^{3+} ($\rho_{\text{Al}^{3+}} = 4.68$). Charge density is an important parameter to interpret the electrophilicity of the metal ions. Higher charge density favours stronger complex-

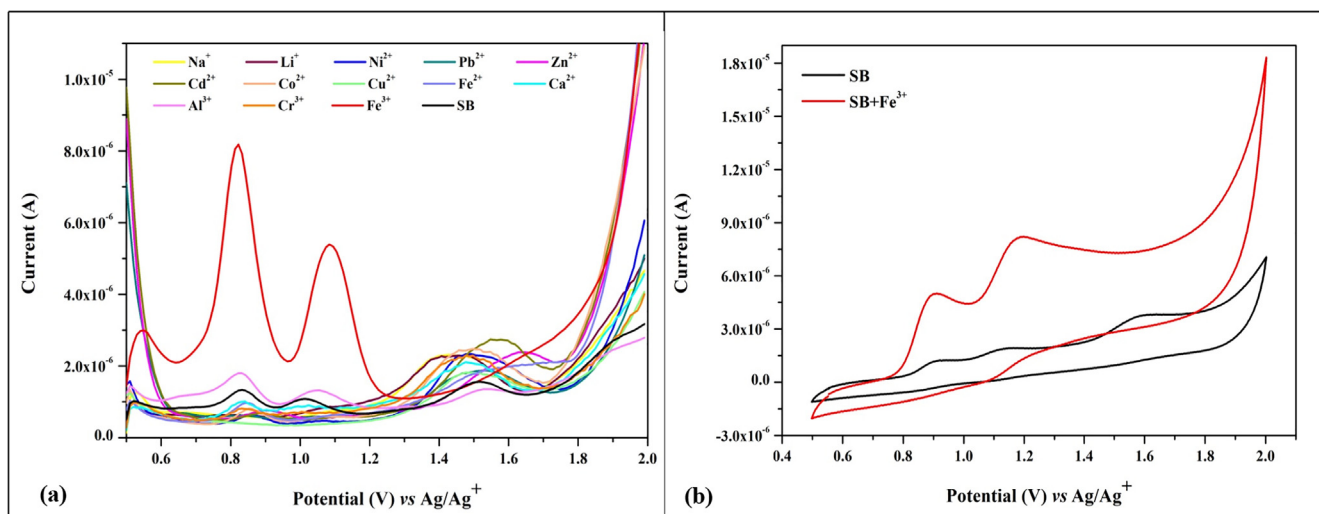


Fig. 2. (a) Differential Pulse Voltammograms (DPV) of receptor SB (5×10^{-4} M in CH_3CN) in the absence and presence of various metal ions. Supporting electrolyte: TBAP (0.01 M), Pulse amplitude: 0.05 V, Pulse width: 0.05 s, Pulse period: 0.5 s; (b) Cyclic Voltammogram (CV) of receptor SB (5×10^{-4} M in CH_3CN) before and after addition of 25 μM addition of Fe^{3+} . Supporting electrolyte: TBAP (0.01 M), Scan rate: 50 mV/sec.

ation with electron rich ligands. This fact rules out the hard metal ions like Na^+ , Li^+ , Ca^{2+} , and Cr^{3+} for favourable complexation with **SB**. Further, out of Fe^{3+} and Al^{3+} , Fe^{3+} exhibit higher standard electrode potential in comparison to Al^{3+} ($\text{Fe}^{3+}=0.77\text{ V}$; $\text{Al}^{3+}=-1.66\text{ V}$ and facilitate Fe^{3+} to bind strongly with electron rich ligand **SB**. Similar strong and selective complexation of polymer poly(1-amino-5-chloroanthraquinone) with Fe^{3+} has been reported by Huang et.al [37].

3.1.3. Quantitative application for Fe^{3+} sensing

In order to confirm the electrochemical recognition sensitivity of **SB** towards Fe^{3+} ions, the voltammetric titration of **SB** was carried out with Fe^{3+} solution in the potential range from 0.5 to 2.0 V vs. Ag/AgCl. The solution of Fe^{3+} with concentration ranged from 0 to 25 μM was sequentially added into a solution of **SB** ($5 \times 10^{-4}\text{ M}$). The increasing concentration of Fe^{3+} ions in solution significantly influenced the position (potential) and height (peak currents) of peaks observed in differential pulse voltammogram of **SB** as shown in Fig. 3. The anodic peak at 1.50 V got vanished on the successive addition of Fe^{3+} ions up to 6 μM . While the peaks at 1.02 V and 0.83 V gradually reaches to the maximum at 25 μM concentration of Fe^{3+} . Also, the peak at 1.02 V showed a shift towards the more positive potential on the gradual addition of Fe^{3+} demonstrating the complexation of **SB** with Fe^{3+} . The plot of the magnitude of peak current at 0.83 V against the concentration of Fe^{3+} is shown in the inset of Fig. 3. The peak current was found to increase with successive addition of Fe^{3+} and exhibit a linear relationship in the concentration range of 1 μM –19 μM with a correlation coefficient of 0.99. The detection limit of the voltammetric sensor was found to be $5.57 \times 10^{-8}\text{ M}$.

3.1.4. Binding Stoichiometry, stability constant and free energy change

For determining the binding constant (K_a) for the complexation between **SB** and Fe^{3+} , Benesi-Hildebrand (BH) equation (1) was used [38]:

$$\frac{1}{\Delta I_p} = \frac{1}{\Delta I_0} + \frac{1}{K_a \Delta I_0 [\text{Fe(III)}]^n} \quad (1)$$

where, $\Delta I_p = I_{\text{max}} - I$, I_{max} and I represent the current of **SB** ($5 \times 10^{-4}\text{ M}$) in the presence and absence of Fe^{3+} , respectively; $[\text{Fe(III)}]$ represents the molar concentration of Fe^{3+} and n denotes the stoichiometric coefficient. The double reciprocal plot of $1/\Delta I_p$ vs. $1/[\text{Fe}^{3+}]$ using data obtained from DPV measurements was drawn which demonstrated a good linearity ($R^2 = 0.99$) and con-

firmed 1:1 complexation between **SB** and Fe^{3+} (Fig. S5). The K_a and free energy change ($\Delta G = -RT \ln K_a$) were calculated to be $1.01 \times 10^4\text{ M}^{-1}$ and -22.84 kJmol^{-1} , respectively. The larger value of binding constant and negative Gibbs free energy indicated the feasibility of the complex formation between two participants.

3.1.5. Interference study

In order to check the influence of foreign ions present along with Fe^{3+} in the same solution which normally occur in real samples, DPVs of **SB** containing 25 μM of Fe^{3+} ions were recorded in the presence of equal amount (25 μM) of different metal ions such as Na^+ , Li^+ , Ca^{2+} , Ni^{2+} , Zn^{2+} , Cd^{2+} , Co^{2+} , Pb^{2+} , Cu^{2+} , Fe^{2+} , Al^{3+} and Cr^{3+} and it was observed that the anodic potentials and peak currents in DPV plot were not or marginally influenced by the presence of other metal ions showing no interference in the detection of Fe^{3+} (shown in Fig. S6). Therefore, receptor **SB** could serve as a promising voltammetric sensor with excellent selectivity for detection of Fe^{3+} in the presence of diverse metal ions.

3.2. Potentiometric measurements

After confirmation of favourable **SB**- Fe^{3+} complex formation and keeping in view the requirement of on-site monitoring of Fe^{3+} without involving heavy instrumentation, CPE incorporating **SB** as modifier was constructed and applied for potentiometric sensing of Fe^{3+} . In addition, using CPE-**SB** potentiometric sensing of various alkali, alkaline earth, and transition metal ions such as Na^+ , Li^+ , Ca^{2+} , Ni^{2+} , Zn^{2+} , Cd^{2+} , Co^{2+} , Pb^{2+} , Cu^{2+} , Fe^{2+} , Al^{3+} and Cr^{3+} were also examined and the electrode characteristics such as linear range and Nernstian slope so obtained are summarized in Table S1. Results indicated that CPE-**SB** exhibited very inferior potentiometric response for all metal ions tested except Fe^{3+} . The sensor responded to metal ions other than Fe^{3+} with slope much below the Nernstian slope values (in mV/decade) i.e. 19.72, 29.58 and 59.16 for trivalent, divalent and monovalent metal ions, respectively. As CPE-**SB** has shown high sensitivity toward Fe^{3+} only, hence it was decided to study systematically its electrode characteristics such as response time, linear concentration range, Nernstian slope, effect of pH and selectivity.

3.2.1. Electrode characteristics

The potentiometric response of CPE-**SB** for Fe^{3+} in the concentration range from $1.0 \times 10^{-10}\text{ M}$ to $1.0 \times 10^{-2}\text{ M}$ was examined to obtain working concentration range and other electrode characteristics. It was found that CPE-**SB** exhibited a near Nernstian slope of $18.6 \pm 0.2\text{ mV/decade}$ over a wide concentration range of Fe^{3+} from 1.0×10^{-7} to $1.0 \times 10^{-2}\text{ M}$ with a detection limit of $5.0 \times 10^{-8}\text{ M}$. The variation in potentiometric response of CPE-**SB** with concentrations of Fe^{3+} and corresponding calibration graph are shown in Fig. 4. It can be seen that the potential increased with increase in the concentration of Fe^{3+} in solution due to the occupancy of Fe^{3+} in the pseudo cavity of **SB** via interaction with donor O and N atoms.

3.2.2. Effect of pH and response time

The pH dependence of CPE-**SB** was analyzed over a wide pH range of 2.0–10.0 for $1.0 \times 10^{-3}\text{ M}$ Fe^{3+} ions. 1 N HNO_3 and 1 N NaOH solutions were used to adjust the pH of Fe^{3+} solution. Fig. S7 shows the variation in potentiometric response as a function of pH. The potential was found to show marginal change in the pH range of 2.0–7.0. The sharp change in potential at higher pH values may be ascribed to the hydrolysis of Fe^{3+} resulting in the formation of hydroxides [39]. Similar results were obtained when $1.0 \times 10^{-2}\text{ M}$ Fe^{3+} solution was subjected to pH variation in the range 2.0–10.0 followed by potentiometric measurements. There-

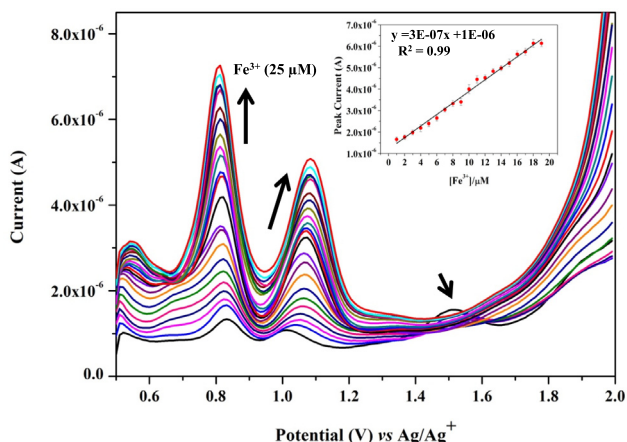


Fig. 3. Differential Pulse Voltammograms (DPV) of receptor **SB** ($5 \times 10^{-4}\text{ M}$ in CH_3CN) in presence of Fe^{3+} ions (0–25 μM). Supporting electrolyte: TBAP (0.01 M), Pulse amplitude: 0.05 V, Pulse width: 0.05 s, Pulse period: 0.5 s. Inset: Calibration plot between $[\text{Fe}^{3+}]$ (1 μM –19 μM) and corresponding peak currents.

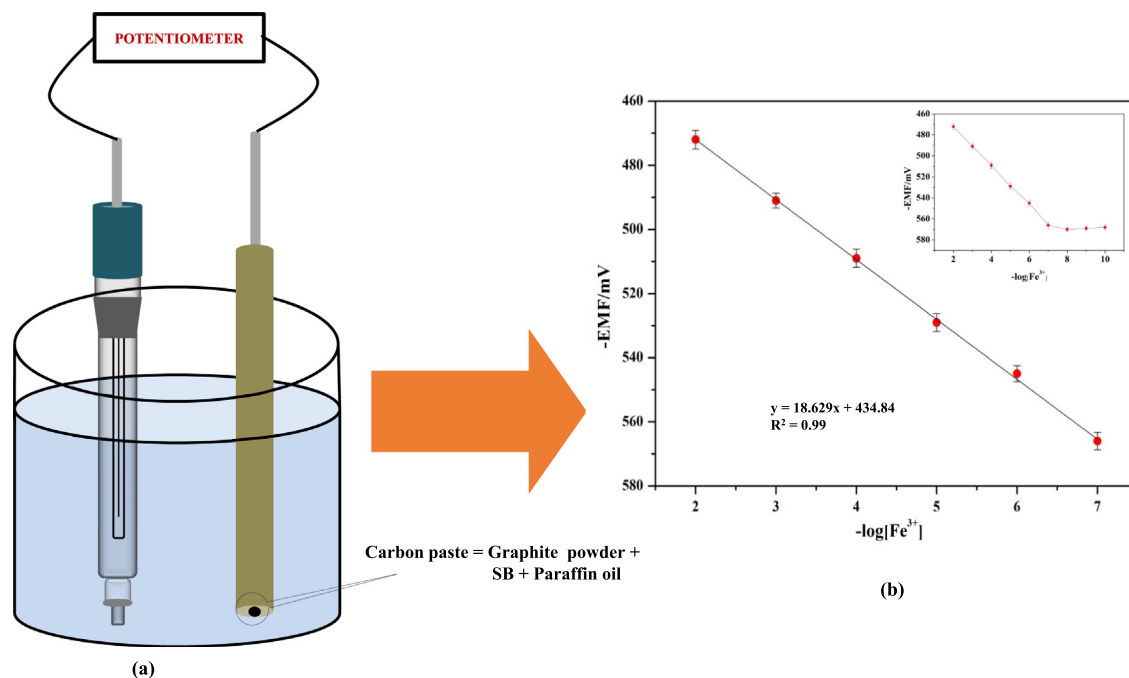


Fig. 4. (a) Schematic representation of potentiometric assembly used for potentiometric sensing using CPE-SB as indicator electrode. (b) Calibration curve of potentiometric response of CPE-SB with variation in $[Fe^{3+}]$. Inset: Potentiometric response of CPE-SB with various concentrations of Fe^{3+} in solution.

fore, pH range 2.0–7.0 can be considered as the working pH range of the CPE-SB

The response time is an average time taken by an electrode to achieve stable potential when it is dipped in successive analyte solutions [40]. For the determination of response time, CPE-SB electrode was subjected to potentiometric measurements in Fe^{3+} solutions in concentration range studied and the corresponding change in potential was observed with respect to time. It was noted that the electrode achieved stable response within 15 s and after which no fluctuations in potential was observed even up to 5 min. Hence, the CPE-SB electrode showed an equilibrium response within 15 s over whole Fe^{3+} concentration range studied.

3.2.3. Selectivity coefficient

The selectivity of CPE-SB was expressed in terms of potentiometric selectivity coefficients ($K_{Fe^{3+},B}$) which represents the response of electrode to the primary ion (Fe^{3+}) in the presence of other ions in the same solution. $K_{Fe^{3+},B}$ were evaluated by using fixed interference method (FIM) [41] using a fixed concentration of secondary ions (1.0×10^{-2} M) in the background and varying the concentration of primary ion Fe^{3+} ranged from 1.0×10^{-10} M to 1.0×10^{-1} M as summarized in Table S2. It was revealed that the selectivity coefficients were in the order of 10^{-3} or lower for almost all the diverse ions tested except univalent ions Na^+ and Li^+ which may be attributed to their charge and these ions may not cause any significant interference in the estimation of Fe^{3+} ions using CPE-SB unless present in large amounts. It can be concluded that CPE-SB could be used for the selective determination of Fe^{3+} by direct potentiometric method even in the presence of foreign ions at higher concentration of 1.0×10^{-2} M.

3.3. Spectroscopic studies supporting SB- Fe^{3+} complex formation

3.3.1. UV-Visible Spectroscopy

In order to confirm the complexation potential of SB with Fe^{3+} using UV-Vis spectroscopy, the absorption spectra of SB ($5 \mu M$ in CH_3CN) was recorded which exhibits distinct bands at 264 and 327 nm (Fig. S8). The band at 264 nm may be attributed to $\pi-\pi^*$

transition of C = N group, while the band at 327 nm corresponds to $n-\pi^*$ transition and intermolecular charge transfer (ICT) in the molecule due to conjugation [42]. Upon addition of Fe^{3+} , the absorption intensity of band at 327 nm was significantly increased (Fig. S8). However, on addition of other metal ions such as Na^+ , Li^+ , Ca^{2+} , Ni^{2+} , Zn^{2+} , Cd^{2+} , Co^{2+} , Pb^{2+} , Cu^{2+} , Fe^{2+} , Al^{3+} and Cr^{3+} , no significant change was observed in absorption intensity of signal at 327 nm. On the other hand, a shoulder appeared at 375 nm in case of Pb^{2+} , Cu^{2+} , Ca^{2+} , Fe^{2+} , Al^{3+} , Cr^{3+} including Fe^{3+} . These changes in absorption spectra i.e. significant enhancement in absorption band at 327 nm confirmed the sensitivity of receptor SB towards Fe^{3+} .

Further, the titration experiment was carried out by the successive addition of Fe^{3+} from 0 to 1.85 equiv. in the solution of receptor SB ($5 \mu M$ in CH_3CN). Upon addition of Fe^{3+} from 0 to 0.15 equiv. a shoulder at 375 nm appeared which might be due to π -electron delocalization (Fig. 5(b)). This shoulder vanished on further addition, while the absorbance band corresponding to 327 nm gradu-

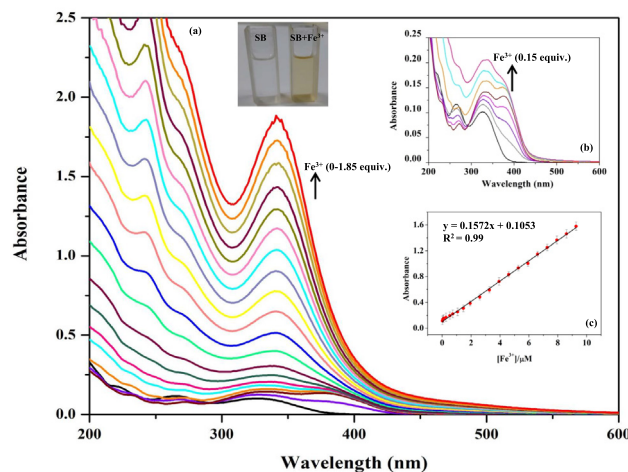


Fig. 5. (a) Absorption behaviour of SB ($5 \mu M$ in CH_3CN) upon successive addition of Fe^{3+} ; (b) enlarged scale showing appearance of new band; (c) Calibration plot of absorbance vs $[Fe^{3+}]$.

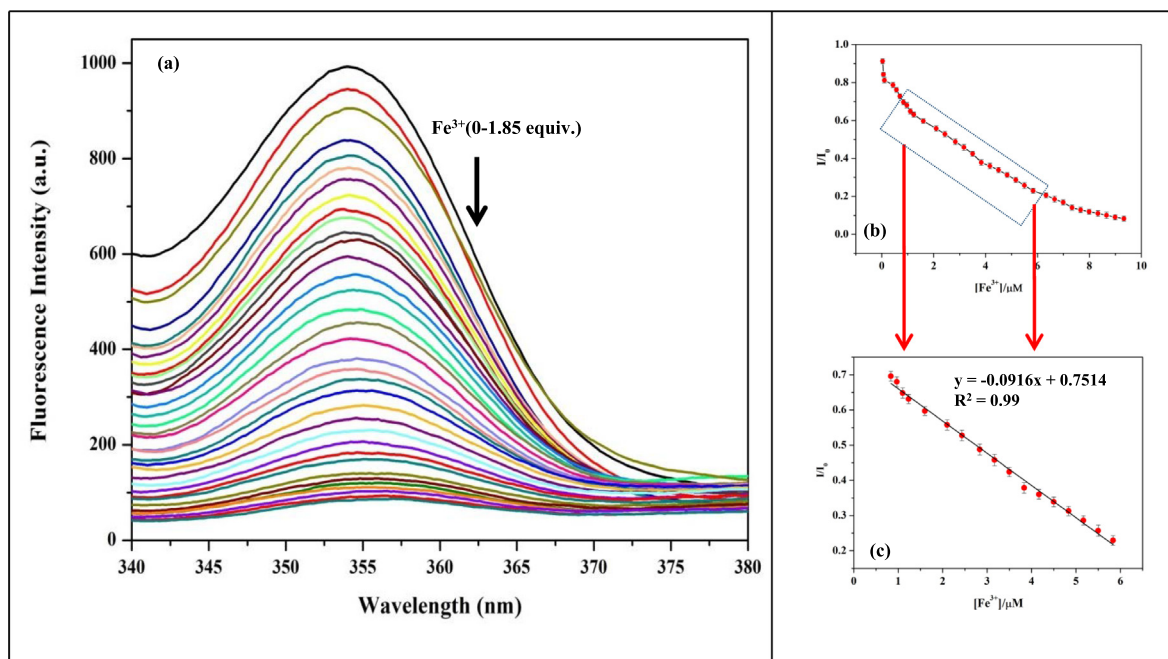


Fig. 6. (a) Emission behaviour of **SB** (5 μM in CH_3CN) upon successive addition of Fe^{3+} ; (b) corresponding change in emission intensity; (c) Calibration plot.

ally increased with successive additions of Fe^{3+} throughout the titration with a red shift from 327 nm to 341 nm (Fig. 5(a)) which may be attributed to ligand to metal charge transfer (LMCT) in **SB**- Fe^{3+} complex. Moreover, there was change in colour from transparent to brown on addition of 1.85 equiv. of Fe^{3+} . The UV-Vis sensor was found to exhibit good linearity in the concentration range of 0.016–9.26 μM and detection limit calculated from the calibration curve (Fig. 5(c)) was found to be 0.56 μM which is far below the recommended WHO limit for iron content in drinking water i.e. 2 mg/L [9].

3.3.2. Fluorescence spectroscopy

The emission behaviour of **SB** (5 μM in CH_3CN) was also investigated using fluorescence measurements at an excitation wavelength of 320 nm. The receptor **SB** displayed an emission band centred at 354 nm which showed a gradual decrease in emission intensity on successive addition of Fe^{3+} up to 1.85 equiv. after which the plateau was achieved (Fig. 6(a)). The plot of fluorescence intensity versus $[\text{Fe}^{3+}]$ was shown in Fig. 6(b). The sensor was found to show response in the linear concentration range of 0.83–5.83 μM and the lowest limit of detection was found to be 0.98 μM ($3\sigma/\text{slope}$). On the other hand, on addition of other alkali, alkaline earth and transition metal ions such as Na^+ , Li^+ , Ca^{2+} , Ni^{2+} , Zn^{2+} , Cd^{2+} , Co^{2+} , Pb^{2+} , Cu^{2+} , Fe^{2+} , Al^{3+} and Cr^{3+} , no apparent alterations in fluorescence spectra were observed (Fig S9). The decrease in emission intensity in the presence of Fe^{3+} may be attributed to the paramagnetic nature of Fe^{3+} which may induce electron/energy transfer processes with fluorophores which may further results in non-radioactive deactivation pathway [43].

Further, 1:1 stoichiometry was confirmed from Job's plot which showed maximum at mole fraction of 0.5 (Fig. S10). Thus, UV-Visible and Fluorescence studies confirmed the discriminating potential of **SB** to detect Fe^{3+} in comparison to other metal ions under investigation.

3.3.3. ^1H NMR and HR-MS studies

To understand the binding behaviour of **SB** with Fe^{3+} , ^1H NMR titrations were also carried out in CH_3CN (d_3) (Fig. S11). All the signals have broadened owing to strong paramagnetic nature of **SB**- Fe^{3+} complex. Moreover, there was a slight downfield shift in signal

of proton of $\text{HC}=\text{N}$ (H_a) along with the splitting of the singlet into doublet which ensures the participation of $\text{C}=\text{N}$ as binding site in complexation of **SB** with Fe^{3+} via imine nitrogens. Furthermore, downfield shift was also observed in signal of proton of methylene group (H_b) (δ 4.47 to 4.51 ppm) which might be attributed to change in electronic environment upon binding of Fe^{3+} with O atoms adjacent to H_b protons. These observations confirm the participation of imine N and O atoms of **SB** in the complex formation with Fe^{3+} .

Further, to gather more information and confirm the binding stoichiometry, mass spectra of **SB** before and after complexation with Fe^{3+} was recorded and a peak at $m/z = 543.1106$ [**SB** + $\text{Fe}^{3+} + \text{K}^+$] $^+$ was observed which corresponds to expected mass of **SB**- Fe^{3+} complex (calculated 504.1500). This analysis confirmed the formation of 1:1 **SB**- Fe^{3+} complex (Fig. S12).

It can be seen that the inferences obtained from spectroscopic measurements such as UV-Visible spectroscopy, fluorescence, NMR and HR-MS provides convincing evidences in support of the major findings achieved from electrochemical techniques i.e. cyclic voltammetry (CV), differential pulse voltammetry (DPV) and potentiometry.

3.4. DFT studies

The molecular orbital analysis was used to explain the sensing behaviour of **SB** towards Fe^{3+} in acetonitrile. The HOMO-LUMO gap represents a key parameter to reflect chemical stability of the molecule before and after binding with Fe^{3+} . As shown in Fig. 7, the HOMO-LUMO gap of **SB** in acetonitrile is 4.11 eV. However, after encapsulating Fe^{3+} , the same energy gap reduces to 1.08 eV. Thus, it can be concluded that **SB**- Fe^{3+} complex is easily formed due to readily accessible energy states owing to the smaller energy gap.

To establish the sensing behaviour of **SB**, TDDFT electronic structure calculations at Frank Codon point were carried out at the optimized geometry of Fe^{3+} encapsulated **SB**. The brightest vertical transitions are between molecular orbitals 115a to 119a and 116a to 119a with 0.0212 oscillatory strength and 3.71 eV excitation energy. The 113b to 120b/121b, 116b to 119b, and 117b to 120b molecular orbital excitations are the second best vertical

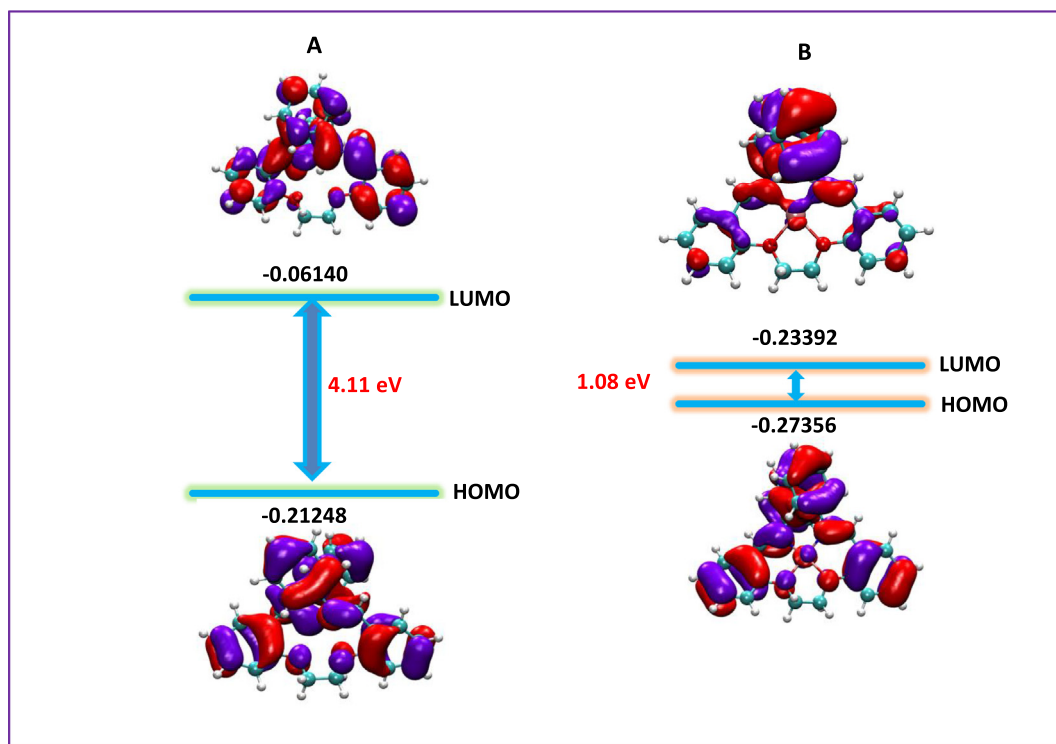


Fig. 7. Pictorial representation of HOMO-LUMO gap of SB before (A) and after (B) encapsulating Fe^{3+} . The HOMO-LUMO values are in atomic units.

transitions with 0.0161 oscillatory strength and 4.90 eV excitation energy. The molecular orbital transition 115a to 119a corresponds to HOMO-3 to LUMO transition whereas the transition 116a to 119a is HOMO-2 to LUMO. According to molecular orbital analysis, HOMO-3 and HOMO-2 are π in nature while as LUMO is located over the aromatic ring as portrayed in Fig. S13. Thus, the above said excitations are mainly π - π^* in nature. Thus, a good agreement was seen between the TDDFT computational studies and inferences obtained from electrochemical and spectroscopic measurements described in previous sections.

3.5. Proposed mechanism

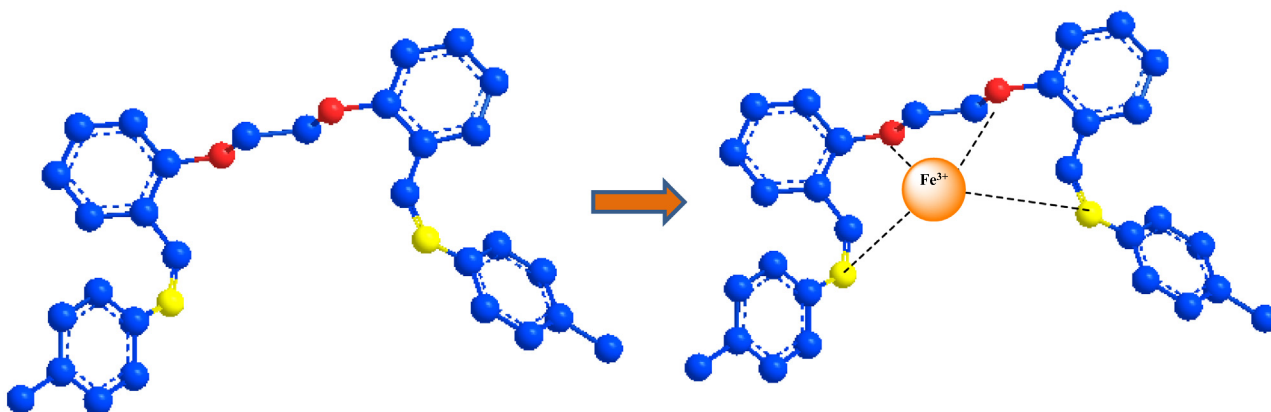
Receptor **SB** is a Schiff base that consists of pseudo cavity which can accommodate metal ions i.e. Fe^{3+} in the present case. It comprises donor units i.e. C = N and O atoms which have the capability to coordinate with metal ion. DPV investigations indicated the increase in peak currents corresponding to peak potentials of imine moieties on increasing concentration of Fe^{3+} which

may be attributed to occupancy of the pseudocavity in **SB** via coordination with enhancement in conduction behaviour of the system (Scheme 2). Similarly, from potentiometric measurements, the potential values increased with Fe^{3+} concentration which justifies the inferences drawn from DPV investigations. Furthermore, it was observed from ^1H -NMR and mass spectra of the **SB-Fe** $^{3+}$ complex that Fe^{3+} possibly interacts with O and C = N units of the molecule and results in the formation of 1:1 complex between **SB** and Fe^{3+} . These investigations lead to the conclusion that Fe^{3+} occupies the pseudo cavity possibly via co-ordination with the donor units in **SB**.

3.6. Analytical application

3.6.1. Potentiometric titration of Fe^{3+} with EDTA

The CPE-**SB** was successfully applied as an indicator electrode to determine Fe^{3+} content from the endpoint in potentiometric titration of Fe^{3+} with EDTA as a titrant. A 25 mL solution of 1.0×10^{-3} M Fe^{3+} was titrated against 1.0×10^{-2} M EDTA solution at pH 6.0. The



Scheme 2. Possible mechanism of coordination responsible for encapsulation of Fe^{3+} in SB.

Table 1
Estimation of Fe³⁺ content in real sample matrices using CPE-SB.

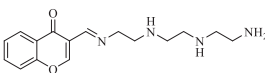
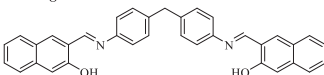
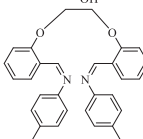
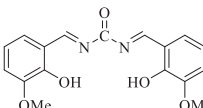
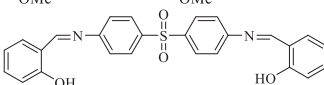
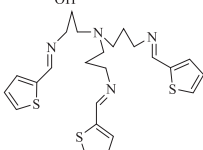
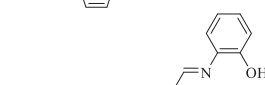
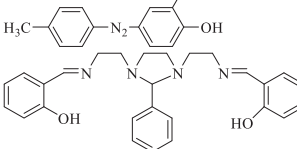
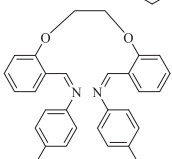
Real Samples		Concentration of Fe ³⁺ (M)		% Compatibility
		CPE-SB sensor	MPAES	
Surface water	Sample 1	8.90×10^{-4} M	8.65×10^{-4} M	102.9%
	Sample 2	9.26×10^{-4} M	9.39×10^{-4} M	98.6%
Ground water	Sample 3	9.37×10^{-4} M	9.58×10^{-4} M	97.8%
	Sample 4	9.67×10^{-4} M	9.74×10^{-4} M	99.2%
Pharmaceutical tablets	Sample 5	5.82×10^{-4} M	5.99×10^{-4} M	97.2%
	Sample 6	5.65×10^{-4} M	5.83×10^{-4} M	96.9%

* All measurements were performed in triplicates.

potential data was plotted against the volume of EDTA added in potentiometric titration and the curve so obtained is shown in Fig. S14. The addition of EDTA causes a decrease in potential which may be attributed to decreased concentration of free Fe³⁺ ions in solution due to their complexation with EDTA and after the end-

point, the potential remains constant due to non-availability or very low concentration of free Fe³⁺ in the solution. The sharp breakpoint corresponds to the completion of Fe³⁺-EDTA complex formation. Hence, the electrode CPE-SB can be used to determine Fe³⁺ content potentiometrically.

Table 2
Comparison of the proposed electrochemical sensors with previously reported Fe³⁺ sensors based on Schiff base.

Voltammetric sensors						
S.No.	Ionophore	Electrode	Linear range	Detection limit	Reference	
1		Glassy Carbon	1.6×10^{-5} to 4.4×10^{-5} M	5.2×10^{-8} M	[25]	
2		SPE	0.625 μ M to 7.5 μ M	0.93 μ M	[26]	
3		Platinum	1–19 μ M	5.57×10^{-8} M	Present work	
Potentiometric sensors						
S.No.	Ionophore	CPE/PVC	Slope (mV/decade)	Linear range (M)	Detection limit (M)	Reference
1		PVC	19.5	3.0×10^{-6} to 1.2×10^{-2}	1.2×10^{-6}	[27]
2		PVC	19.3 \pm 0.6	1.0×10^{-7} to 1.0×10^{-2}	7.4×10^{-8}	[28]
3		PVC	19.8 \pm 0.3	1.0×10^{-2} to 1.0×10^{-8}	8.3×10^{-9}	[44]
4		PVC	28.5 (\pm 0.5)	3.5×10^{-6} to 4.0×10^{-2}	$2.5 (\pm 0.1) \times 10^{-6}$	[45]
5		PVC	20.0	6.3×10^{-6} to 1.0×10^{-1}	5.0×10^{-6}	[46]
6		CPE	18.6 \pm 0.2	1.0×10^{-7} - 1.0×10^{-2}	5.0×10^{-8}	Present work

3.6.2. Real sample analysis

In order to explore the real applicability of the proposed CPE-SB, it was applied for determination of Fe^{3+} content in real sample matrices i.e. ground water, surface water and pharmaceutical samples and the results so obtained are presented in Table 1. It was found that the proposed sensors could determine Fe^{3+} content in real samples accurately. Moreover, the results were also compared with a well-established technique Microwave Plasma Atomic Emission Spectroscopy (MPAES) and were found to be in good agreement (Table 1). Thus, the proposed method proved its candidature for the estimation of Fe^{3+} content in different environmental and biological samples after suitable pre-treatment if required. Moreover, for analysis of environmental samples such as ground-water and surface water, it offers additional advantages such as portability, no sample pre-treatment and on-site monitoring.

3.7. Comparison with literature

In recent years, there have been an extensive reports utilizing Schiff based ionophores for spectroscopic and electrochemical detection for Fe^{3+} . Attempts have been made to compare the performance of proposed SB based voltammetric and potentiometric Fe^{3+} sensors with previously reported Fe^{3+} ion-selective sensors (Table 2). There have been only two reports for voltammetric detection of Fe^{3+} using schiff based ionophores which showed comparable or inferior detection limits i.e. 5.2×10^{-8} M [25] and $0.93 \mu\text{M}$ [26] in comparison to that of SB based voltammetric sensor i.e. 5.57×10^{-8} M. As far as potentiometric sensors for Fe^{3+} are concerned, many reports of Schiff based ion-selective electrodes are available in literature but most of them involve PVC membrane as matrix for supporting the ionophore and are associated with their own limitations but no report on Fe^{3+} -CPE incorporating Schiff base is found. To the best of our knowledge, present work is the first report of Schiff base incorporated in CPE for potentiometric determination of Fe^{3+} . Moreover, potentiometric sensor based on SB was found to exhibit better or comparable detection limit than other ion-selective electrodes utilizing Schiff based ionophore [25,27,28,45,46] except the potentiometric sensor reported by Zamani *et al.* [44]. In addition, CPEs offers additional advantages of renewability, low ohmic resistance, easy modification, good response and no need of any internal reference solution in comparison to previously reported PVC membrane electrodes for detection of Fe^{3+} thus making CPE-SB more expedient.

SB was also explored for spectroscopic detection of Fe^{3+} using UV-visible and fluorescence and found to give satisfactory results. An attempt was also made to compare the performance of SB for spectroscopic sensing of Fe^{3+} with the previous reports (Table S3). It can be seen that the proposed SB based spectroscopic sensors exhibit comparable or even better detection limits than most of the previously reported sensors employing similar techniques viz. UV-Visible [29,30,47] and fluorescence [31,49-54] except for one reported by Sun *et al.* [48].

Moreover, it can be concluded that SB based electrochemical sensors reported in present work exhibited better detection limits as compared to many of the previous reports utilizing Schiff based ionophore molecules.

4. Conclusions

Schiff base ionophore 1,1'-((ethane-1,2-diylbis(oxy))bis(2,1-phenylene))bis(N-p-tolylmethanimine) (SB) was synthesized and successfully applied for selective voltammetric and potentiometric detection of Fe^{3+} with acceptable detection limits of 5.57×10^{-8} M and 5.0×10^{-8} M, respectively followed by confirmation of binding behaviour of SB with Fe^{3+} using UV-Visible and Fluorescence

measurements. The coordination mechanism was validated by DFT, ^1H NMR and mass spectroscopy. The characteristic performance of the proposed SB based sensor is found to be comparable or even superior as compared to previously reported Fe^{3+} sensors. CPE-SB was subjected to real analytical application and successfully applied as an indicator electrode for determination of Fe^{3+} in real sample matrices such as surface water, ground water and pharmaceutical tablets with great precision and accuracy. The application of the proposed sensors could be extended for determination of Fe^{3+} content in food crops, biological (blood, urine) and environmental (water, soil) samples.

Declaration of Competing Interest

The authors declare that they have no known competing financial interests or personal relationships that could have appeared to influence the work reported in this paper.

Acknowledgements

The authors acknowledge the financial support from the Science & Engineering Research Board, Department of Science and Technology (SERB-DST), New Delhi and Ministry of Human Resources Development, Government of India under RUSA 2.0 Programme. The first author (SK) is thankful to Department of Science and Technology under PURSE (69919/Estt./A-11) and CSIR-SRF (09/254(0306)/2020-EMR-I) for the fellowship.

Appendix A. Supplementary data

Supplementary data to this article can be found online at <https://doi.org/10.1016/j.molliq.2021.115954>.

References

- [1] K. Shikama, The molecular mechanism of autoxidation for myoglobin and hemoglobin: a venerable puzzle, *Chem. Rev.* 98 (1998) 1357–1374.
- [2] C.D. Kaplan, J. Kaplan, Iron acquisition and transcriptional regulation, *Chem. Rev.* 109 (2009) 4536–4552.
- [3] N. Abbaspour, R. Hurrell, R. Kelishadi, Review on iron and its importance for human health, *Journal of research in medical sciences: the official journal of Isfahan University of Medical Sciences* 19 (2014) 164–174.
- [4] E.C. Theil, D.J. Goss, Living with iron (and oxygen): questions and answers about iron homeostasis, *Chem. Rev.* 109 (2009) 4568–4579.
- [5] E.S. Gurzau, C. Neagu, A.E. Gurzau, Essential metals—case study on iron, *Ecotoxicol. Environ. Saf.* 56 (2003) 190–200.
- [6] E. Beutler, V. Felitti, T. Gelbart, N. Ho, Genetics of iron storage and hemochromatosis, *Drug Metab. Dispos.* 29 (2001) 495–499.
- [7] L. Zecca, M.B. Youdim, P. Riederer, J.R. Connor, R.R. Crichton, Iron, brain ageing and neurodegenerative disorders, *Nat. Rev. Neurosci.* 5 (2004) 863–873.
- [8] D.T. Dexter, F.R. Wells, A.J. Lee, F. Agid, Y. Agid, P. Jenner, C.D. Marsden, Increased nigral iron content and alterations in other metal ions occurring in brain in Parkinson's disease, *J. Neurochem.* 52 (1989) 1830–1836.
- [9] WHO, Iron in drinking-water. Background document for preparation of WHO Guidelines for drinking-water quality, Geneva, World Health Organization (WHO/SDE/WSH/03.04/08) (2003).
- [10] M. Vuori, Direct and indirect effects of iron on river ecosystems, In *Annales Zoologici Fennici* (pp. 317–329). Finnish Zoological and Botanical Publishing Board. 1995, January.
- [11] E.J. Parra, P. Blondeau, G.A. Crespo, F.X. Rius, An effective nanostructured assembly for ion-selective electrodes. An ionophore covalently linked to carbon nanotubes for Pb^{2+} determination, *Chem. Commun.* 47(2011) 2438–2440.
- [12] S.J. Bora, R. Dutta, S. Ahmed, D.J. Kalita, B. Chetia, Experimental cum theoretical study of cryptand derivative having high selectivity and sensitivity towards Zn ion, *J. Mol. Struct.* 1194 (2019) 178–186.
- [13] D. Vlascici, E. Fagadar-Cosma, I. Popa, V. Chiriac, M. Gil-Agusti, A novel sensor for monitoring of iron (III) ions based on porphyrins, *Sensors* 12 (2012) 8193–8203.
- [14] C. Göde, M.L. Yola, A. Yilmaz, N. Atar, S. Wang, A novel electrochemical sensor based on calixarene functionalized reduced graphene oxide: application to simultaneous determination of Fe (III), Cd (II) and Pb (II) ions, *J. Colloid Interface Sci.* 508 (2017) 525–531.

- [15] R. Aminameli, M.H. Fekri, H. Shafie, M. Darvishpour, H. Khanmohammadi, Application of a New Macrocylic-PVC Electrode to Potentiometric Studies of Fe (III) Ion, *J. Phys. Theor. Chem.* 9 (2012) 209–213.
- [16] R. Sharma, M. Chhibber, S.K. Mittal, A new ionophore for chemical sensing of F^- , CN^- and Co^{2+} using voltammetric, colorimetric and spectrofluorimetric techniques, *RSC Adv.* 6 (2016) 51153–51160.
- [17] M.A. Deshmukh, M. Gicevicius, A. Ramanaviciene, M.D. Shirsat, R. Viter, A., Ramanavicius, Hybrid electrochemical/electrochromic Cu (II) ion sensor prototype based on PANI/ITO-electrode, *Sens. Actua. B Chem.*, 248 (2017) 527–535.
- [18] H.L. Siddiqui, A. Iqbal, S. Ahmad, W. Weaver, Synthesis and spectroscopic studies of new Schiff bases, *Molecules* 11 (2006) 206–211.
- [19] K.B. Kim, H. Kim, E.J. Song, S. Kim, I. Noh, C. Kim, A cap-type Schiff base acting as a fluorescence sensor for zinc(II) and a colorimetric sensor for iron(II), copper(II), and zinc(II) in aqueous media, *Dalton Trans.* 42 (2013) 16569–16577.
- [20] M.N. Abbas, H.S. Magar, Highly sensitive and selective solid-contact calcium sensor based on Schiff base of benzil with 3-aminosalicylic acid covalently attached to polyacrylic acid amide for health care, *J. Solid State Electrochem.* 22 (2018) 181–192.
- [21] W. Al Zoubi, N. Al Mohanna, Membrane sensors based on Schiff bases as chelating ionophores—A review, *Spectrochim. Acta A Mol. Biomol.* 132 (2014) 854–870.
- [22] N.M. Hosny, M.A. Hussien, F.M. Radwan, N. Nawar, Synthesis, spectral characterization and DNA binding of Schiff-base metal complexes derived from 2-amino-3-hydroxypropanoic acid and acetylacetone, *Spectrochim. Acta A Mol. Biomol.* 132 (2014) 121–129.
- [23] A.L. Berhanu, I. Mohiuddin, A.K. Malik, J.S. Aulakh, V. Kumar, K.H. Kim, A review of the applications of Schiff bases as optical chemical sensors, *Trends Anal. Chem.* 116 (2019) 74–91.
- [24] L. Wang, M. Xu, Y. Xie, C. Qian, W. Ma, L. Wang, Y. Song, Ratiometric electrochemical glucose sensor based on electroactive Schiff base polymers, *Sens. Actua. B Chem.* 285 (2019) 264–270.
- [25] S.K. Mittal, S. Kumar, N. Kaur, Enhanced Performance of CNT-doped Imine Based Receptors as Fe (III) Sensor Using Potentiometry and Voltammetry, *Electroanal.* 31 (2019) 1229–1237.
- [26] S.K. Mittal, S. Rana, N. Kaur, C.E. Banks, A voltammetric method for Fe (III) in blood serum using a screen-printed electrode modified with a Schiff base ionophore, *Analyst* 143 (2018) 2851–2861.
- [27] B. Shafaatian, S.O. Sadati, A. Soleymannpour, F. Amouzad, Highly selective solid contact sensor for low level concentration measurements of iron (III) in pharmaceutical and biological media, *J. Anal. Chem.* 73 (2018) 1202–1208.
- [28] H.A. Zamani, M.R. Ganjali, M. Salavati-Niasari, Fabrication of an iron (III)-selective PVC membrane sensor based on a bis-bidentate Schiff base ionophore, *Transit. Met. Chem.* 33 (2008) 995–1001.
- [29] T.G. Jo, K.H. Bok, J. Han, M.H. Lim, C. Kim, Colorimetric detection of Fe^{3+} and Fe^{2+} and sequential fluorescent detection of Al^{3+} and pyrophosphate by an imidazole-based chemosensor in a near-perfect aqueous solution, *Dyes Pigm.* 139 (2017) 136–147.
- [30] D.Y. Patil, A.A. Patil, N.B. Khadke, A.V. Borhade, Highly selective and sensitive colorimetric probe for Al^{3+} and Fe^{3+} metal ions based on 2-aminoquinolin-3-yl phenyl hydrazone Schiff base, *Inorg. Chim. Acta* 492 (2019) 167–176.
- [31] C. Pan, K. Wang, S. Ji, H. Wang, Z. Li, H. He, Y. Huo, Schiff base derived Fe^{3+} -selective fluorescence turn-off chemosensors based on triphenylamine and indole: synthesis, properties and application in living cells, *RSC Adv.* 7 (2007) 36007–36014.
- [32] L. Lan, Q. Niu, Z. Guo, H. Liu, T. Li, Highly sensitive and fast responsive “turn-on” fluorescent sensor for selectively sensing Fe^{3+} and Hg^{2+} in aqueous media based on an oligothiophene derivative and its application in real water samples, *Sens. Actua. B Chem.* 244 (2007) 500–508.
- [33] L. Cui, J. Wu, H. Ju, Electrochemical sensing of heavy metal ions with inorganic, organic and bio-materials, *Biosens. Bioelectron.* 63 (2015) 276–286.
- [34] S. Ilhan, H. Temel, A. Kilic, Synthesis and characterization of new macrocyclic Cu(II) complexes from various diamines, copper(II) nitrate and 1,4-bis(2-formylphenoxy)butane, *Chinese J. Chem.* 25 (2007) 1547–1550.
- [35] G. Chopra, N. Chopra, D. Kaur, Elucidating the intermolecular hydrogen bonding interaction of proline with amides—quantum chemical calculations, *Struct. Chem.* 30 (2019) 755–767.
- [36] A. Kamal, R. Raj, V. Kumar, R.K. Mahajan, Highly selective amide-tethered 4-aminoquinoline- β -lactam based electrochemical sensors for Zn (II) ion recognition, *Electrochim. Acta* 166 (2015) 17–25.
- [37] S. Huang, P. Du, C. Min, Y. Liao, H. Sun, Y. Jiang, Poly (1-amino-5-chloroanthraquinone): highly selective and ultrasensitive fluorescent chemosensor for ferric ion, *J. Fluoresc.* 23 (2013) 621–627.
- [38] S. Kumar, S.K. Mittal, N. Kaur, R. Kaur, Improved performance of Schiff based ionophore modified with MWCNT for Fe (II) sensing by potentiometry and voltammetry supported with DFT studies, *RSC Adv.* 7 (2017) 16474–16483.
- [39] A. Kamal, N. Kumar, V. Bhalla, M. Kumar, R.K. Mahajan, Rhodamine-dimethyliminocinnamyl based electrochemical sensors for selective detection of iron (II), *Sens. Actua. B-Chem.* 190 (2014) 127–133.
- [40] H. Khani, M.K. Rofouei, P. Arab, V.K. Gupta, Z. Vafaei, Multi-walled carbon nanotubes-ionic liquid-carbon paste electrode as a super selectivity sensor: application to potentiometric monitoring of mercury ion (II), *J. Hazard. Mater.* 183 (2010) 402–409.
- [41] Y. Umezawa, K. Umezawa, H. Sato, Selectivity coefficients for ion-selective electrodes: recommended methods for reporting K_A , Bpot values (Technical Report), *Pure Appl. Chem.* 67 (1995) 507–518.
- [42] C. Lee, W. Yang, R.G. Parr, Development of the Colle-Salvetti correlation-energy formula into a functional of the electron density, *Phys. Rev. B* 37 (1988) 785.
- [43] B. Zhao, T. Liu, Y. Fang, L. Wang, B. Song, Q. Deng, Two ‘turn-off’ Schiff base fluorescence sensors based on phenanthro [9, 10-d] imidazole-coumarin derivatives for Fe^{3+} in aqueous solution, *Tetrahedron Lett.* 57 (2016) 4417–4423.
- [44] H.A. Zamani, M.R. Ganjali, F. Faridbod, M. Salavati-Niasari, Heptadentate Schiff-base based PVC membrane sensor for Fe (III) ion determination in water samples, *Mater. Sci. Eng., C* 32 (2012) 564–568.
- [45] M.H. Mashhadizadeh, I.S. Shoaie, N. Monadi, A novel ion selective membrane potentiometric sensor for direct determination of Fe, (III) in the presence of Fe (II), *Talanta* 64 (2004) 1048–1052.
- [46] V.K. Gupta, A.K. Jain, S. Agarwal, G. Maheshwari, An iron (III) ion-selective sensor based on a μ -bis (tridentate) ligand, *Talanta* 71 (2007) 1964–1968.
- [47] N. Łukasik, E. Wagner-Wysiecka, Salicylaldehyde-based receptor as a material for iron (III) selective optical sensing, *J. Photochem. Photobiol.* 346 (2017) 318–326.
- [48] T. Sun, N. Qingfen, L. Yang, L. Tianduo, L. Haixia, Novel oligothiophene-based dual-mode chemosensor: “naked-eye” colorimetric recognition of Hg^{2+} and sequential off-on fluorescence detection of Fe^{3+} and Hg^{2+} in aqueous media and its application in practical samples, *Sens. Actua. B-Chem.* 248 (2017) 24–34.
- [49] L. Wang, X. Yang, X. Chen, Y. Zhou, X. Lu, C. Yan, Y. Xu, R. Liu, J. Qu, A novel fluorescence probe based on triphenylamine Schiff base for bioimaging and responding to pH and Fe^{3+} , *Mater. Sci. Eng., C* 72 (2017) 551–557.
- [50] S. Hasan, N.A. Hamedan, A.A. Razali, N.H. Uyup, H.M. Zaki, Synthesis and characterization of p-dimethylaminobenzaldehyde benzoylthiourea and study towards selective and sensitive fluorescent sensor for detection of iron (III) cation in aqueous solution, In IOP Conference Series: Mater. Sci. Eng. 172 (2017) 012050.
- [51] G. Singh, J. Sindhu, V. Kumar, V. Sharma, S.K. Sharma, S.K. Mehta, M.H. Mahnashi, A. Umar, R. Kataria, Development of an off-on selective fluorescent sensor for the detection of Fe^{3+} ions based on Schiff base and its Hirshfeld surface and DFT studies, *J. Mol. Liq.* 296 (2019) 111814.
- [52] Z. Zuo, X. Song, D. Guo, Z. Guo, Q. Niu, A dual responsive colorimetric/fluorescent turn-on sensor for highly selective, sensitive and fast detection of Fe^{3+} ions and its applications, *J. Photochem. Photobiol.* 382 (2019) 111876.
- [53] G. Dong, K. Duan, Q. Zhang, Z. Liu, A new colorimetric and fluorescent chemosensor based on Schiff base-phenyl-crown ether for selective detection of Al^{3+} and Fe^{3+} , *Inorg. Chim. Acta* 487 (2019) 322–330.
- [54] J. Harathi, K. Thenmozhi, AIE-active Schiff base compounds as fluorescent probes for the highly sensitive and selective detection of Fe^{3+} ions, *Mater. Chem. Front.* 4 (2020) 1471–1482.